ACS APPLIED MATERIALS & INTERFACES

Research Article

Cite This: ACS Appl. Mater. Interfaces 2018, 10, 19940−19947

www.acsami.org

Zinc Oxide-Enhanced Piezoelectret Polypropylene Microfiber for Mechanical Energy Harvesting

Jianxiong Zhu,*[,†,⊥] Yali Zhu,[‡] Weixing Song,[§,†] Hui Wang,[†,∥] Min Gao,[⊥] Minkyu Cho,[⊥] and Inkyu Park*[,⊥]

[†]Beijing Institute of Nanoenergy and Nanosystems, Chinese Academy of Sciences, National Center for Nanoscience and Technology (NCNST), Beijing 100083, China

[‡]Guangdong Province Traditional Chinese Medical Hospital, Guangzhou 510120, Guangdong, China

[§]Department of Chemistry, Capital Normal University, Beijing 100048, China

[∥]The Key Laboratory of Low-carbon Chemistry and Energy Conservation of Guangdong Province, School of Chemistry, Sun Yat-sen University, Guangzhou 510275, China

[⊥]Department of Mechanical Engineering, Korea Advanced Institute of Science and Technology (KAIST), 291 Daehak-ro, Yuseong-gu, Daejeon 34141, Republic of Korea

Supporting Information

ABSTRACT: This paper reports zinc oxide (ZnO)-coated piezoelectret polypropylene (PP) microfibers with a structure of two opposite arc-shaped braces for enhanced mechanical energy harvesting. The ZnO film was coated onto PP microfibers via magnetron sputtering to form a ZnO/PP compound structure. Triboelectric Nanogenerator (TENG) based on ZnO/PP microfiber compound film was carefully designed with two opposite arc-shaped braces. The results of this study demonstrated that the mechanical energy collection efficiency of TENG based on piezoelectret PP microfiber was greatly enhanced by the coated ZnO and high-voltage corona charging method. We found that, with the step-increased distance of traveling for the movable carbon black electrode, an electrical power with an approximately quadratic function of distance was generated by this mechanical−electrical energy conversion, because more PP microfibers were connected to the electrode. Further, with a full contact condition, the peak of the generated voltage, current, and charges based on the ZnO/PP microfibers by this mechanical−electrical energy conversion with 1 m/s^2 reached 120 V, 3 μA, and 49 nC, respectively. Moreover, a finger-tapping test was used to demonstrate that the ZnO/PP microfiber TENG is capable of lighting eight light-emitting diodes.

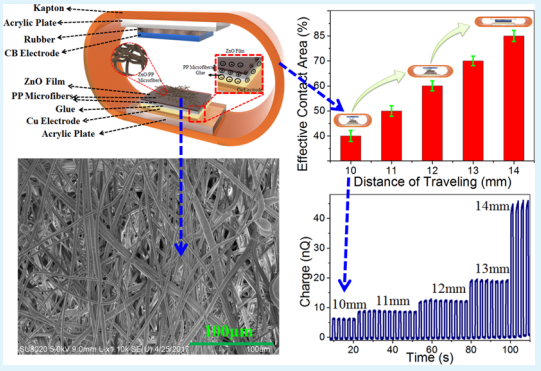

KEYWORDS: *microfiber for energy harvester, PP piezoelectret, triboelectric nanogenerator, ZnO/PP compound film, arc-shaped braces structure*

1. INTRODUCTION

Wearable electronics contribute greatly to the development of human interactive applications that enrich our daily lives. However, the conventional chemical battery has some significant constraints on the rapid development of wearable electronics due to its limited life span and environmentally unfriendly nature.[1−3] There are several promising methods, which can be used to provide energy to these electronic devices, such as piezoelectric, electrostatic, electromagnetic, and triboelectric energy harvesting.[4−7] Among the various potential technologies, the triboelectric method is considered to be one of the most appropriate solutions and has attracted much research interest, because it has the advantage of higher voltage output than that of other methods. Triboelectric Nanogenerator (TENG) was invented in 2012; since then, TENG quickly developed on the basis of the electrostatic effect and contact electrification physics. The major principle of the TENG is based on the contact and separation of two different materials. The interactive potential voltage drives electrons to flow back and forth through the external load.[7−9] Moreover, TENG directly converts mechanical energy into electricity from wind, flowing water, and human motion on the basis of triboelectricity and the electrostatic induction effect.[9−11]

A lot of effort has been dedicated by many research groups to improve the electrical output performance of TENGs through new material syntheses, advanced structural designs, mechanical-coupling effects, and so on. Polymers, such as poly(vinylidene fluoride) (PVDF), polypropylene (PP), polyimide, and poly(phenylene sulfide), have attracted extensive interest due to their intrinsic advantages, including high breakdown

Received: February 8, 2018
Accepted: May 22, 2018
Published: May 22, 2018

DOI: 10.1021/acsami.8b02458
ACS Appl. Mater. Interfaces 2018, 10, 19940−19947

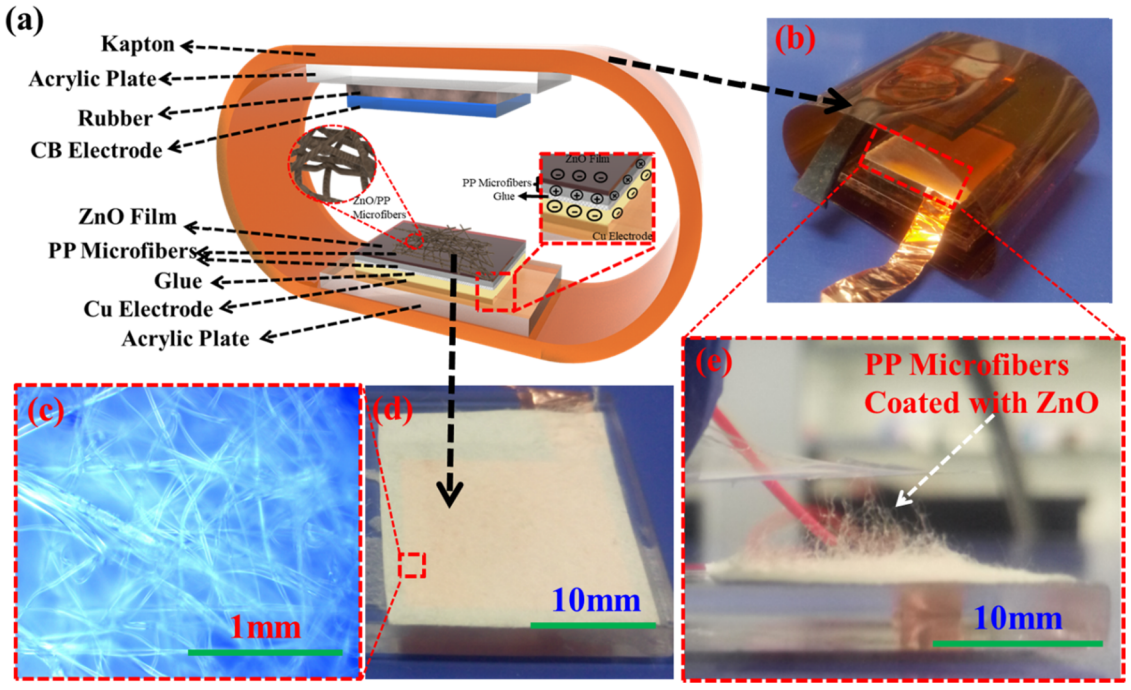

Figure 1. (a) The schematics and (b) the prototype of ZnO/PP microfiber nonwoven mat-based TENG system, (c) the optical microscope image of the ZnO-coated PP microfiber, (d) the top view, and (e) the side view of the ZnO-coated PP microfiber.

strength, facile processability, low dielectric loss, and lightness, which make them an excellent option for the TENG application.[12−20] Lu et al. reported a novel and facile fabrication poling-free dynamic PVDF−Nafion polymeric piezoelectret generator with 14.6 V/cm^2 output. The weakness of their research was focused on the stimulated force and did not deal with the precharging onto their reported device resulted a small voltage outcome.[13] Lin et al. introduced PVDF nanofiber webs for mechanical energy harvesting using short-distance electrospinning.[17] They took advantage of higher delamination resistance, tensile strength, and breakdown strength in PVDF for robust mechanical−electrical energy conversion. PP is one of the most attractive candidates for a biocompatible, nontoxic, and cost-effective polymer dielectric and also has higher charge-holding properties than those of the other polymer matrices.[21−32] These remarkable properties make PP-based materials the optimal choice for the energy-harvesting application. For example, Jang et al. reported a PP/graphene oxide nanofiber that can generate energy density as high as 12.6 J/cm^3.[21] Even though their research took advantage of the high breakdown electric field in PP matrix, the potential application of the composite film in energy harvesting was still limited for the applications. Sahraoui et al. introduced an enhancement of energy-harvesting performance of PP electret using a corona discharge system.[22] However, the designed prototype could only achieve power below 13.93 nW, which made it inapplicable in real applications. Sessler et al. reported the dielectric cross-linked PP that can be significantly intensified using the surface functionalization of PP.[24] The prototype in this paper generated power up to 120 μW with a load resistance of 9 MΩ, whereas the cross-linked PP stack still had constrained application areas compared with PP microfiber. Wang et al. reported a 48% enhancement of electrical performance of TENG through a prior-charge injection method with the PDVF and Nylon film.[25] However, there is still room to improve its electrical performance based on the coupling of the piezoelectric/piezoelectret/triboelectric mechanisms for energy harvesting. In this paper, we propose a TENG system based on zinc oxide (ZnO)-coated piezoelectret PP microfiber with a structure of two opposite arc-shaped braces for enhanced mechanical energy-harvesting characteristics. We demonstrate that the piezoelectret PP microfiber greatly enhances the collection efficiency of mechanical energy harvesting using ZnO coating and high-voltage corona charging. Furthermore, with a full contact condition, the peak of the generated voltage, current, and charges based on the ZnO/PP microfiber were 120 V, 3 μA, and 49 nC, respectively, at 1 m/s^2. Moreover, we demonstrate that finger-tapping motion on this TENG device is capable of lighting eight light-emitting diodes (LEDs).

2. EXPERIMENTAL SECTION

Figure 1a schematically depicts the three-dimensional structure of the reported TENG system, whereas Figure 1b shows a real image of TENG. It is a multilayer structure with two separated components. The bottom component contains an acrylic substrate with a dimension of 2 cm × 2 cm × 2 mm, which was prepared by a laser cutting machine, a copper electrode tape with a dimension of 2 cm × 2 cm × 0.1 mm, a PP microfiber nonwoven mat (Nangong Hualong Felt Products Co., Ltd.) of ∼0.2 mm thickness (see Figure 1c−e), and a decorated ZnO film. The ZnO film was coated onto the PP microfiber nonwoven mat by magnetron-sputtering equipment (PVD 75 Pro Line Kurt J. Lesker Company) for 15 min. The top component contains another piece of an acrylic substrate with a dimension of 2 cm × 2 cm × 2 mm and a layer of carbon black (CB) electrode film. This film was made of silicone rubber (Smooth-On Ecoflex 00-30) and carbon black powders (TIMCAL Super P Li Company) with a volume ratio of 1:1. A glass stick was used for the aid of mechanical stirring for 45 min in a cup, and then the mixture was carefully poured onto a flat acrylic plate to form the conductive thin film. Subsequently, the flat plate with the CB conductive mixture thin film was placed into a 70 °C vacuum box to evaporate the water solvent. A piece of polyimide film with a dimension of 10 cm × 2.5 cm × 0.125 mm was prepared to attach those two separate parts to form a pair of arc-shaped braces. Note that the arc-shaped braces function as a mechanical spring to suspend the

DOI: 10.1021/acsami.8b02458
ACS Appl. Mater. Interfaces 2018, 10, 19940−19947

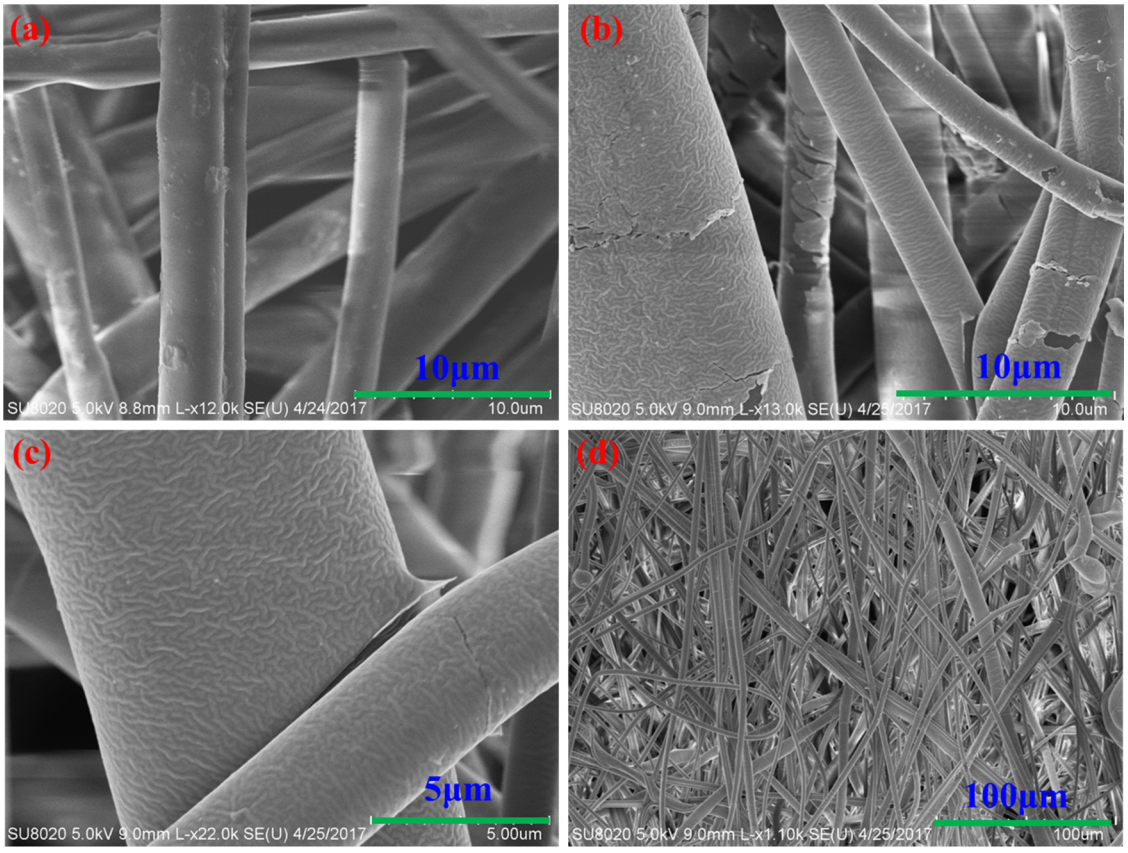

Figure 2. Characterization of materials by SEM analysis: (a) the morphology of PP microfibers without ZnO coating, (b) the morphology of PP microfibers coated with ZnO at the same scale of view, (c) a close-up view of the intercrossed PP microfibers with ZnO coating, and (d) morphology the ZnO/PP microfiber in a relatively large area.

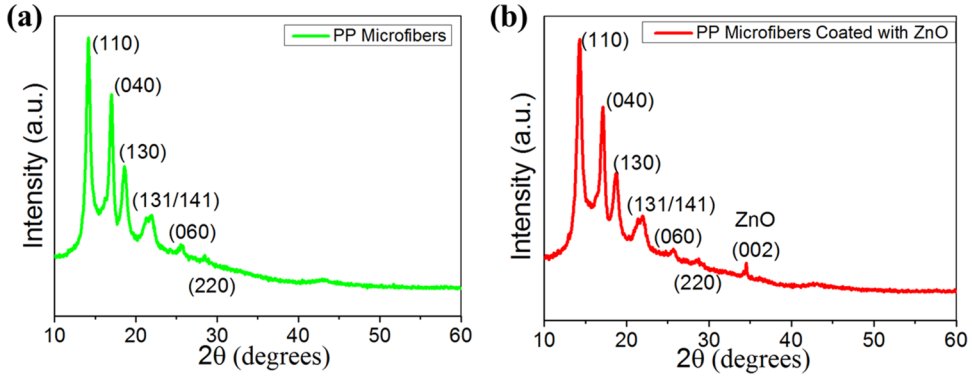

Figure 3. Wide-angle X-ray diffraction patterns for (a) PP microfibers without ZnO and (b) PP microfibers coated with ZnO.

top component. The initial air gap of the designed prototype was measured as ~14 mm. Finally, lead wires were connected to each of the electrodes (bottom copper electrode and top CB electrode) for the electrical measurement. The generated power was obtained by the triboelectric contact between the top CB electrode and the PP microfiber. During the electrical measurement, the bottom copper electrode and the top CB electrodes were always connected, respectively, to the positive and the negative terminals of an electrometer for the data acquisition. It should be noted that the PP microfibers coated with ZnO were subjected to high negative charges (high-voltage polarization apparatus, Model ET-2673A) at room temperature for 5 min with a voltage of −6 kV (see Figure S1a). To better demonstrate the charged PP microfibers piezoelectret,[22,24,25,33−35] fluorinated ethylene propylene (FEP) was used as a separated component to attract the charged PP microfibers (see Figure S1b). We found that more effective contact area (i.e., the total surface of the PP fibers contacting the FEP film) is created when the FEP film is pushed to approach the bottom PP microfiber nonwoven mat.

3. RESULTS AND DISCUSSION

The surface morphology of the PP microfibers with and without ZnO coating was characterized by the scanning electron microscope (SEM, Hitachi SU-8020) as shown in Figure 2. Figure 2a depicts the PP microfibers without ZnO coating, whereas the ZnO-coated PP microfiber nonwoven mat at the same scale can be observed in Figure 2b. The average thickness of the ZnO film was estimated as ~200 nm based on the deposition rate and time. Figure 2c gives a close-up view of the intercrossed PP microfibers with ZnO coating, and Figure 2d illustrates the morphology of ZnO/PP microfiber in a

DOI: 10.1021/acsami.8b02458
ACS Appl. Mater. Interfaces 2018, 10, 19940−19947

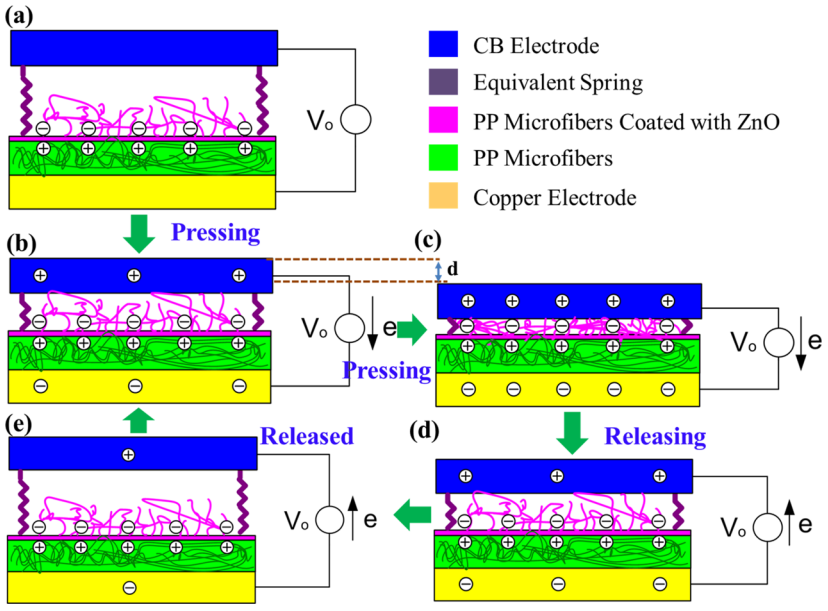

Figure 4. Working principle of the TENG system based on PP microfibers coated with ZnO film: (a) initial state, (b) contact state with short distance of traveling, (c) contact state with large distance of traveling, (d) releasing state, and (e) released state.

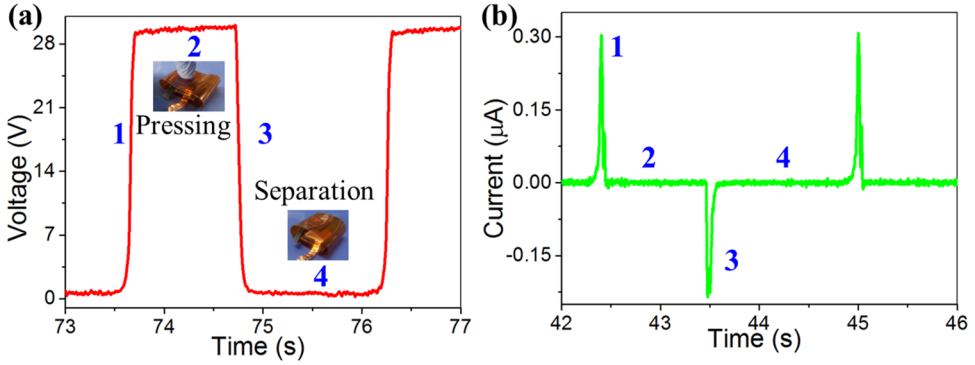

Figure 5. Measurement results for the enhanced ZnO-coated PP microfiber TENG: (a) open-circuit voltage V_{oc}, a = 1 m/s^2 and (b) short-circuit current I_{sc}, a = 1 m/s^2.

relatively large area. Note that the PP microfibers were used to make contact with the CB electrode directly to generate the electricity. The crystal structure of the PP microfibers without and with ZnO was characterized with X-ray diffraction (PANalytical, X'pert3 powder), and the results are shown in Figure 3a,b, respectively. It indicated that the crystalline-type PP microfiber had peaks at 2θ that were 13.9, 16.6, 18.2, 21.6, 23.9, and 28.9°, which correspond to the planes (110), (040), (130), (131/141), (060), and (220), respectively. In addition, when the PP microfiber was coated with ZnO, a peak at 34.2° (002) was observed due to the element of ZnO coated on the PP microfibers. In the diffraction spectra, there was a shift in the (002) plane to smaller angles (θ = 34.2°) compared to the standard angle (34.43°).[30] This indicates a compressive residual stress in the ZnO film. It should also be noted that the other crystalline planes of ZnO were barely observed due to much smaller peaks compared with those of the crystalline PP microfibers.

Figure 4 schematically displays the working principle of the ZnO-coated PP microfiber-based TENG system. Figure 4a is the initial condition or the separated state. When the top CB electrode plate is driven to move closer to the bottom PP microfiber nonwoven mat, the potential voltage on the electrodes dramatically increases due to more contact area between the PP microfibers and the top CB electrode (see Figure 4b,c). If the external force is dismissed, the voltage on the electrode dramatically decreases because of less effective contacting area between the PP microfibers and the top CB electrode (see Figure 4d,e). The potential voltage in the process of separation and near contact of the electret PP (see Figure S2a,b) was obtained from a finite element analysis (FEA) simulation performed by COMSOL Multiphysics. Under an ideal condition, we found that, with smaller gap between the top movable carbon black (CB) electrode and the bottom PP microfiber electret film, more power was generated by this mechanical–electrical energy conversion because more PP microfibers were connected with the electrode. The open-circuit voltage (V_{oc}) and the short-circuit current (I_{sc}) of the prototype with the operation are described in Figure 5. The "starting" contact between the bottom PP microfibers and the top CB electrode is defined with a number "1", and the "constant" pause is defined with a number "2". Number "3" indicates the "beginning of the releasing" state between the bottom PP microfibers and the top CB electrode. Number "4" denotes the fully separated state. It should be noted that the electrons on the electrodes transfer to the load resistor due to

DOI: 10.1021/acsami.8b02458
ACS Appl. Mater. Interfaces 2018, 10, 19940–19947

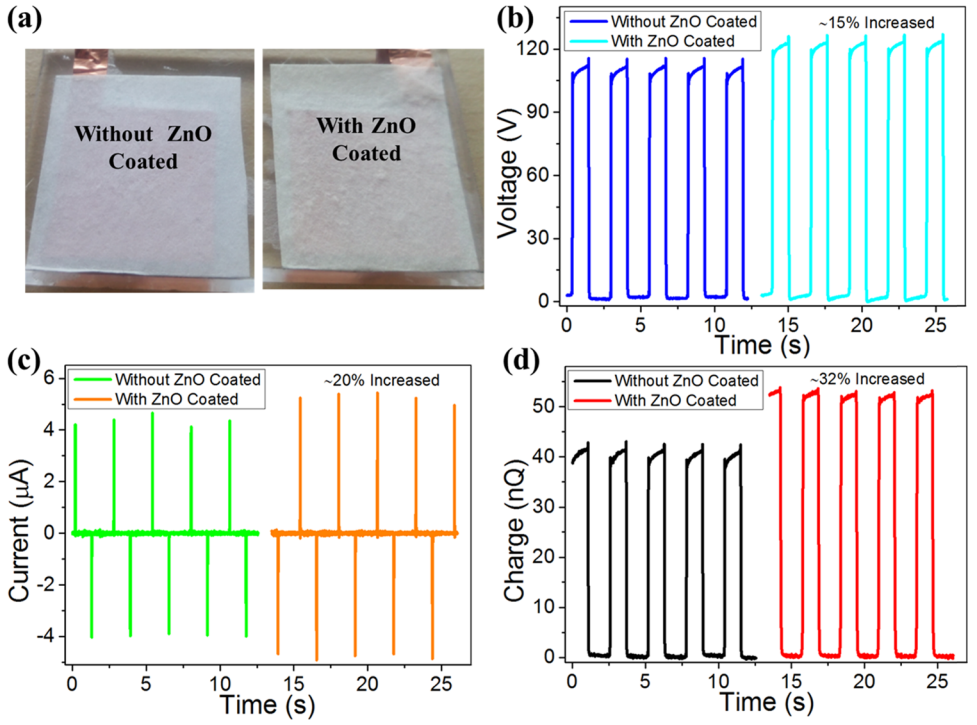

Figure 6. Comparison between PP microfibers without and with ZnO: (a) real image of the pp microfibers with and without coated ZnO; (b) V_{oc}, a = 1 m/s^2; (c) I_{sc}, a = 1 m/s^2; and (d) Q_{oc}, a = 1 m/s^2.

the electrostatic equilibrium of PP microfiber and the top CB electrode.

When the deformation is made through an external force acting on the TENG, the generated open-circuit voltage (V_{oc}) between the electrodes is given as

$$V_{oc} = \frac{Q_{sc}}{C} = \frac{2\sigma x}{\varepsilon_r} \quad (1)$$

where ε_r is the dielectric constant, σ is the triboelectric charge density on the PP microfiber, and x is the instantaneous gap between the two separated surfaces. Thus, the capacitance of the TENG is determined by

$$C = \frac{\varepsilon_0 \varepsilon_r S}{d} \quad (2)$$

where ε_0 is the dielectric constant in a vacuum, S is the effective contact area between the top CB electrode and the bottom PP microfiber nonwoven mat, and d is the compressed deformation (the distance of traveling) of the movable top CB electrode (see Figure S3).

To analyze the distinction between the PP microfibers with and without ZnO coating, a linear motor was used to conduct a standard periodical contact test, and the collected results are shown in Figure 6. Here, a linear motor (LinMot, Inc., Elkhorn, WI) was used to provide the periodical motion to the device, and an electrometer (Keithley 6514, Keithley Instruments, Inc., Ohio) connected to a computer was used to measure the open-circuit voltage (V_{oc}), short-circuit current (I_{sc}), and accumulated charge (Q_{oc}). The data were recorded through a LabVIEW program in a real time. Figure 6a shows the real image of PP microfibers prototype with and without coated ZnO. Figure 6b–d illustrate the electrical performance measurement of the prototype with and without ZnO coating by the linear motor with an acceleration of 1 m/s^2. The results revealed that the coating of PP microfibers with ZnO increased V_{oc}, I_{sc}, and Q_{oc} by ~15, ~20, and ~32%, respectively. Figure S4 demonstrates why ZnO/PP microfiber was chosen as the triboelectric material in our TENG device. Compared with pure PTFE, the ZnO/PP microfiber achieved 50% increases of the generated charges. Moreover, we found that, with corona charging onto the ZnO/PP materials, the generated charges exhibited a 52% further increase from ZnO/PP, whereas the electrification time decreased dramatically.

To investigate the mechanical energy conversion effect of the PP microfibers coated with ZnO, we gradually increased the distance of traveling to the top movable CB electrode component using a linear motor for the measurement shown in Figures 7 and S5. We found that, with the step-increased distance of traveling, the peak value of the short-circuit current (I_{sc}) and the peak value of the open-circuit voltage (V_{oc}) significantly increased with approximately a quadratic relationship corresponding to the value of the distance of traveling for the movable top CB electrode. Figure 7d shows the results of dependence between the step-increased distance of traveling and the generated peak charges. The maximum value of V_{oc}, I_{sc}, and Q_{oc} reached 120 V, 3 μA, and 45 nQ, respectively, in a fully contacted state. Figure S6 depicts the relationship between the step-increased distance of traveling and the percentage of effective contacting area for ZnO/PP microfibers and the movable top CB electrode. Table S1 shows the comparison of output voltage and transfer charges in our study and the current state-of-the-art results. We found that our triboelectric-based energy harvester generated output voltage almost 10 times higher than those of piezoelectric-based[15,17] energy harvesters. Compared with triboelectric-based energy harvester,[23] our piezoelectret/triboelectric device can obtain ~5 times higher voltage and ~7 times higher charge than the former device. We confirmed that our study had much higher transfer charges compared with the results of previously published study. To

DOI: 10.1021/acsami.8b02458
ACS Appl. Mater. Interfaces 2018, 10, 19940–19947

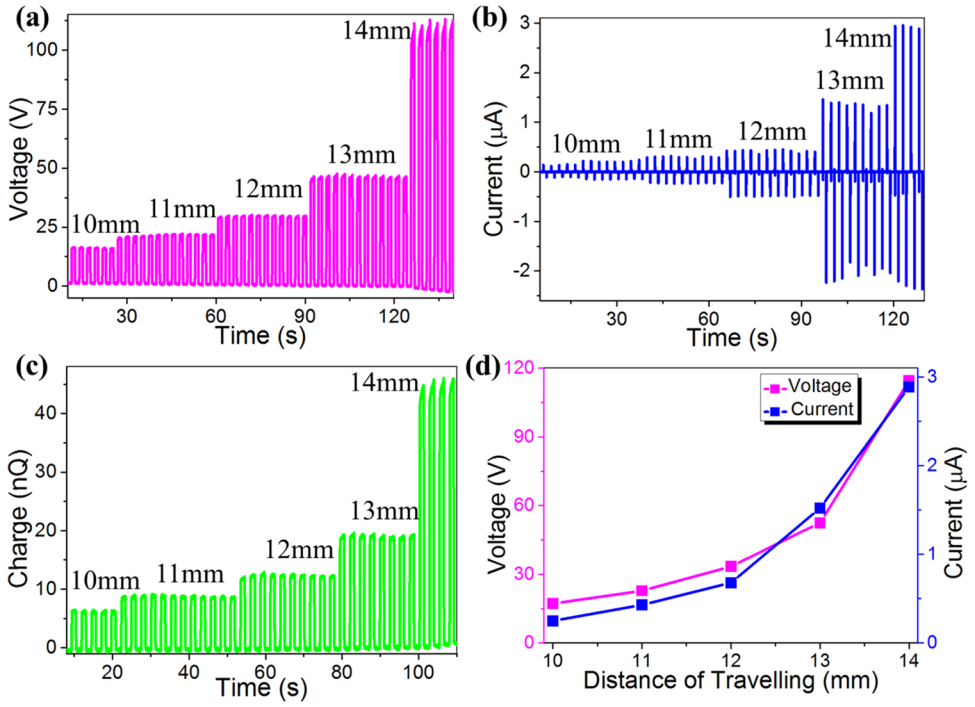

Figure 7. Measurement results on the correlation between the electrical characterization of the TENG system and the step-increased distance of traveling for the movable CB electrode components. (a) V_{oc}, (b) I_{sc}, (c) Q_{oc}, and (d) the relationship for the step-increased distance of traveling with V_{oc} and I_{sc}.

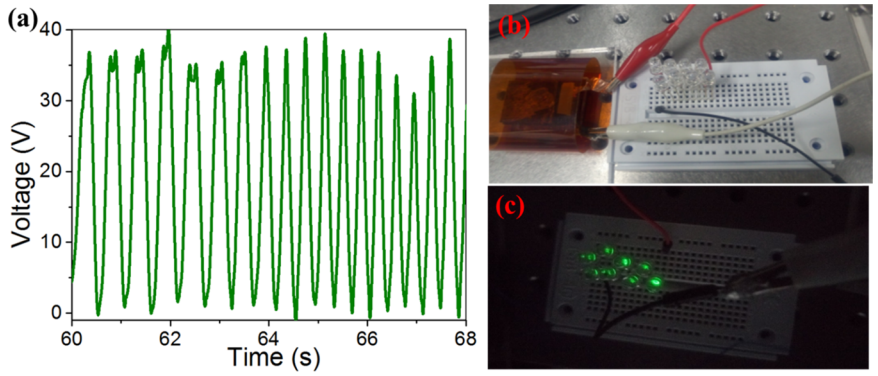

Figure 8. Finger-tapping application: (a) the real-time V_{oc} value under periodical finger tapping, (b) the prototype connected with eight LED lights, and (c) the lit LEDs.

demonstrate the reliability and durability of our device, V_{oc} and I_{sc} in the prototype were measured for more than 1600 s (~750 cycles). Figure S7 shows that there was no evident degradation after a long-term continuous operation, which confirmed the robust reliability and durability of our device.

A finger-tapping test was used to demonstrate the application of mechanical energy conversion of our TENG system (see Figure 8). When a finger continuously tapped onto the device, the open-circuit voltage (V_{oc}) was measured to demonstrate the instantaneous transfer charges between the top CB electrode and the bottom copper electrode. The generated voltage is displayed in Figure 8a, and the generated power was capable of lighting eight LEDs as shown in Figure 8b,c.

4. CONCLUSIONS

This study proposed a TENG system using ZnO-coated piezoelectret PP microfibers with a structure of two opposite arc-shaped braces to enhance mechanical energy harvesting. The results demonstrated that the piezoelectret ZnO/PP microfibers greatly enhanced the collection efficiency of mechanical energy by ZnO coating and a high-voltage corona charging method. Under the full contact condition and an acceleration of 1 m/s^2, the peak of the generated voltage, current, and charges of the ZnO/PP microfiber-based TENG device reached 120 V, 3 μA, and 49 nC, respectively. Moreover, a random mechanical energy-harvesting test using finger tapping demonstrated the electrical performance of the TENG that is capable of lighting eight LEDs. This composite ZnO-coated piezoelectret polypropylene (PP) microfiber can have various applications, such as motion driven energy harvesting, self-powered pressure force sensing, and self-powered strain sensing, due to its advantages: high transfer charge, high output voltage, and big coupling ZnO/PP surface area of microfibers. Furthermore, the easy fabrication and high efficiency of this device will be very useful in IoT systems that require sensing nodes with self-power generation.

DOI: 10.1021/acsami.8b02458
ACS Appl. Mater. Interfaces 2018, 10, 19940−19947

■ ASSOCIATED CONTENT

Supporting Information

The Supporting Information is available free of charge on the ACS Publications website at DOI: 10.1021/acsami.8b02458.

Corona charge onto PP microfibers coated with ZnO and the zoom out of charged PP microfibers; PP microfibers were subjected with fluorinated ethylene propylene film. It shows the strong electrostatic effect to the PP microfibers. FEA simulation of potential voltage with 0.4 cm gap; FEA simulation of triboelectric potential voltage with 0.1 cm gap. The ZnO/PP microfibers TENG device, the optical image with an initial state and the optical image with a pressed state, and the schematic graph with an initial state and the schematic graph with a pressed state. Generated electrical charges for comparison between PTFE and ZnO/PP microfibers. Measurement results of the relationship between the step-increased distance of traveling and the generated peak charges. The step-increased distance of traveling with the percent of contact of the PP microfibers. Comparison of the output voltage and transfer charges in our study and the current state-of-the-art. V_{oc} and I_{sc} were to measure for more than 1600 s (PDF)

■ AUTHOR INFORMATION

Corresponding Authors

*E-mail: danverzhu@gmail.com. Tel: +82-42-350-5253 (J.Z.).
*E-mail: inkyu@kaist.ac.kr. Tel: +82-42-350-3240 (I.P.).

ORCID

Jianxiong Zhu: 0000-0002-9172-5255
Weixing Song: 0000-0002-7880-053X
Minkyu Cho: 0000-0002-0006-2063
Inkyu Park: 0000-0001-5761-7739

Notes

The authors declare no competing financial interest.

■ ACKNOWLEDGMENTS

This study was funded by Shenzhen Science and Technology Innovation Committee (No. GRCK2016082914424352) and National Research Foundation of Korea (No. 2015R1A5A1037668). The authors declare that there is no conflict of interest with this publication.

■ REFERENCES

(1) Song, H. J.; Choi, Y.; Wereley, N. M.; Purekar, A. S. Energy Harvesting Devices using Macro-fiber Composite Materials. *J. Intell. Mater. Syst. Struct.* **2010**, *21*, 647−658.

(2) Ramadan, K. S.; Sameoto, D.; Evoy, S. A Review of Piezoelectric Polymers as Functional Materials for Electromechanical Transducers. *Smart Mater. Struct.* **2014**, *23*, 1−26.

(3) Zhao, J.; You, Z. A Shoe-embedded Piezoelectric Energy Harvester for Wearable Sensors. *Sensors* **2014**, *14*, 12497−12510.

(4) Anton, S.; Farinholt, K.; Erturk, A. Piezoelectret Foam-based Vibration Energy Harvesting. *J. Intell. Mater. Syst. Struct.* **2014**, *25*, 1681−1692.

(5) Li, H.; Tian, C.; Deng, Z. D. Energy Harvesting from Low Frequency Applications using Piezoelectric Materials. *Appl. Phys. Rev.* **2014**, *1*, No. 041301.

(6) Shi, Y. G.; Wang, Y. C.; Mei, D. Q.; Feng, B.; Chen, Z. C. Design and Fabrication of Wearable Thermoelectric Generator Device for Heat Harvesting. *IEE Robotics and Automation Letters* **2018**, *3*, 373−378.

(7) Ki, H. S.; Kim, J. H.; Kim, J. A Review of Piezoelectric Energy Harvesting Based on Vibration. *Int. J. Precis. Eng. Manuf.* **2014**, *12*, 1129−1141.

(8) Wang, Z. L.; Wu, W. Nanotechnology-Enabled Energy Harvesting for Self-Powered Micro-/Nanosystems. *Angew. Chem., Int. Ed.* **2012**, *51*, 11700−11721.

(9) Yang, Y.; Zhang, H.; Zhong, X.; Yi, F.; Yu, R.; Zhang, Y.; Wang, Z. L. Electret Film-Enhanced Triboelectric Nanogenerator Matrix for Self-Powered Instantaneous Tactile Imaging. *ACS Appl. Mater. Interfaces* **2014**, *6*, 3680−3688.

(10) Shi, X.; Zhou, W.; Ma, D.; Ma, Q.; Bridges, D.; Ma, Y.; Hu, A. Electrospinning of Nanofibers and Their Applications for Energy Devices. *J. Nanomater.* **2015**, *2015*, 1−20.

(11) Zhang, L.; Cheng, L.; Bai, S.; Su, C.; Chena, X.; Qin, Y. Controllable Fabrication of Ultrafine Oblique Organic Nanowire Arrays and their Application in Energy Harvesting. *Nanoscale* **2015**, *7*, 1285−1289.

(12) Huang, F. L.; Wang, Q. Q.; Wei, Q. F.; Gao, W. D.; Shou, H. Y.; Jiang, S. D. Dynamic Wettability and Contact angles of Poly (vinylidene fluoride) Nanofiber Membranes Grafted with Acrylic Acid. *eXPRESS Polym. Lett.* **2010**, *4*, 551−558.

(13) Xu, C. W.; Zhang, Lei.; Xu, Y. L.; Yin, Z. Z.; Chen, Q.; Ma, S. Y.; Zhang, H. H.; Huang, R.; Zhang, C. L.; Jin, L.; Yang, W. Q.; Lu, J. Filling the holes in piezopolymers with a solid electrolyte: a new paradigm of poling-free dynamic electrets for energy harvesting. *J. Mater. Chem. A* **2017**, *5*, 189−200.

(14) Liu, W.; Cheng, X.; Fu, X.; Stefanini, C.; Dario, P. Preliminary Study on Development of PVDF Nanofiber based Energy Harvesting Device for an Artery Microrobot. *Microelectron. Eng.* **2011**, *88*, 2251−2254.

(15) Liu, Z. H.; Pan, C. T.; Lin, L. W.; Huang, J. C.; Ou, Z. Y. Direct-write PVDF Nonwoven Fiber Fabric Energy Harvesters via the Hollow Cylindrical Near-field Electrospinning Process. *Smart Mater. Struct.* **2014**, *23*, No. 025003.

(16) Priya, S. Advances in Energy Harvesting using Low Profile Piezoelectric Transducers. *J. Electroceram.* **2017**, *19*, 167−184.

(17) Shao, H.; Fang, J.; Wang, H.; Lang, C.; Lin, T. Robust Mechanical-to-Electrical Energy Conversion from Short- Distance Electrospun Poly (vinylidene fluoride) Fiber Webs. *ACS Appl. Mater. Interfaces* **2015**, *7*, 22551−22557.

(18) Shao, H.; Fang, J.; Wang, H.; Lang, C.; Yan, G.; Lin, T. Mechanical Energy-to-Electricity Conversion of Electron/Hole-Transfer Agent-Doped Poly (Vinylidene Fluoride) Nanofiber Webs. *Macromol. Mater. Eng.* **2017**, *302*, No. 1600451.

(19) Sheikh, F. A.; Cantu, T.; Macossay, J.; Kim, H. Fabrication of Poly (vinylidene fluoride) (PVDF) Nanofibers Containing Nickel Nanoparticles as Future Energy Server Materials. *Sci. Adv. Mater.* **2011**, *3*, 216−222.

(20) Zhang, S.; Yan, B.; Luo, Y.; Miao, W.; Xu, M. An Enhanced Piezoelectric Vibration Energy Harvesting System with Macro Fiber Composite. *Shock Vib.* **2015**, *2015*, No. 916870.

(21) Cho, S.; Kim, M.; Lee, J. S.; Jang, J. Polypropylene/Polyaniline Nanofiber/Reduced Graphene Oxide Nanocomposite with Enhanced Electrical, Dielectric, and Ferroelectric Properties for a High Energy Density Capacitor. *ACS Appl. Mater. Interfaces* **2015**, *7*, 22301−22314.

(22) Eddiai, A.; Meddad, M.; Guyomar, D.; Hajjaji, A.; Boughaleba, Y.; Yuse, K.; Sahraoui, B.; Touhtouh, S. Enhancement of Electrostrictive Polymer Efficiency for Energy Harvesting with Cellular Polypropylene Electrets. *Synth. Met.* **2012**, *162*, 1948−1953.

(23) Gu, G. Q.; Han, C. B.; Tian, J. J.; Lu, C. X.; He, C.; Jang, T.; Wang, Z. L.; Li, Z. Antibacterial Composite Film-Based Triboelectric Nanogenerator for Harvesting Walking Energy. *ACS Appl. Mater. Interfaces* **2017**, *9*, 11882−11888.

(24) Zhang, X.; Wu, L.; Sessler, G. M. Energy Harvesting from Vibration with Cross-linked Polypropylene Piezoelectrets. *AIP Adv.* **2015**, *5*, No. 077185.

(25) Wang, Z.; Cheng, L.; Zheng, Y.; Qin, Y.; Wang, Z. L. Enhancing the Performance of Triboelectric Nanogenerator through Prior-charge

DOI: 10.1021/acsami.8b02458
ACS Appl. Mater. Interfaces 2018, 10, 19940−19947

Injection and its Application on Self-powered Anticorrosion. *Nano Energy* **2014**, *10*, 37−43.
(26) Wei, X. Y.; Zhu, G.; Wang, Z. L. Surface-charge Engineering for High-performance Triboelectric Nanogenerator based on Identical Electrification Materials. *Nano Energy* **2014**, *10*, 83−89.
(27) Helseth, L. E.; Guo, X. D. Contact Electrification and Energy Harvesting Using Periodically Contacted and Squeezed Water Droplets. *Langmuir* **2015**, *31*, 3269−3276.
(28) Jeong, B. W.; Kim, M. O.; Lee, J. I.; Eun, Y. K.; Choi, J. W.; Kim, J. B. Development of MEMS Multi-Mode Electrostatic Energy Harvester Based on the SOI Process. *Micromachines* **2017**, *8*, 51−55.
(29) Yang, Z. C.; Halvorsen, E.; Dong, T. Power Generation from Conductive Droplet Sliding on Electret Film. *Appl. Phys. Lett.* **2012**, *100*, No. 213905.
(30) Silva, E. P. D.; Chaves, M.; Silva, G. J. D.; Arruda, L. B. D.; Lisboa-Fiho, P. N.; Durrant, S. F.; Bortoleto, J. R. R. Al-doping Effect on the Surface Morphology of ZnO Films Grown by Reactive RF Magnetron Sputtering. *Mater. Sci. Appl.* **2013**, *4*, 761−767.
(31) Saravanakumar, B.; Mohan, R.; Thiyagarajan, K.; Kim, S. J. Fabrication of a ZnO Nanogenerator for Eco-friendly Biomechanical Energy Harvesting. *RSC Adv.* **2013**, *3*, 16646−16656.
(32) Yang, W. Q.; Chen, J.; Zhu, G.; Wen, X. N.; Bai, P.; Su, Y. J.; Lin, Y.; Wang, Z. L. Harvesting Vibration Energy by a Triple-cantilever based Triboelectric Nanogenerator. *Nano Res.* **2013**, *6*, 880−886.
(33) Li, F. B.; Sebastian, J. M.; Jones, M. E. Processing Aids for Webs, Including Electret Webs. European Patent 10759281.8, September 11, 2016.
(34) Tao, H. In situ Charging Fiber Spinning Method for Producing a Nonwoven Electret. US Patent 8871011B2, May 26, 2016.
(35) Kilic, A.; Shim, E.; Pourdeyhimi, B. Electrostatic Capture Efficiency Enhancement of Polypropylene Electret Filters with Barium Titanate. *Aerosol Sci. Technol.* **2015**, *49*, 666−673.

DOI: 10.1021/acsami.8b02458
ACS Appl. Mater. Interfaces 2018, 10, 19940−19947